Theiler, R., & Zuber, H. (1984) *Hoppe-Seyler's Z. Physiol. Chem. 365*, 721-729.
Tinoco, I., Jr. (1962) *Adv. Chem. Phys. 4*, 113-157.
Varga, A. R., & Staehlin, L. A. (1985) *J. Bacteriol. 161*, 921-927.
Wiemken, V., & Bachofen, R. (1982) *Biochim. Biophys. Acta 681*, 72-76.
Wiemken, V., & Bachofen, R. (1985) *Physiol. Veg. 23*, 789-800.
Wiemken, V., Brunisholz, R., Zuber, H., & Bachofen, R. (1983) *FEMS Lett. 16*, 297-301.
Yphantis, D. A. (1964) *Biochemistry 3*, 297-317.
Zuber, H. (1986) *Encycl. Plant Physiol., New Ser. 19*, 238-251.
Zuber, H., Sidler, W., Füglistaller, P., Brunisholz, R., & Theiler, R. (1985) in *Molecular Biology of the Photosynthetic Apparatus* (Steinback, K. E., et al., Eds.) pp 183-196, Cold Spring Harbor Laboratory, Cold Spring Harbor, NY.

Nitric Oxide Adducts of the Binuclear Iron Site of Hemerythrin: Spectroscopy and Reactivity†

Judith M. Nocek and Donald M. Kurtz, Jr.*
Department of Chemistry, Iowa State University, Ames, Iowa 50011
J. Timothy Sage, Yao-Min Xia, and Peter Debrunner
Department of Physics, University of Illinois, Urbana, Illinois 61801
Andrew K. Shiemke, Joann Sanders-Loehr, and Thomas M. Loehr
Department of Chemical and Biological Sciences, Oregon Graduate Center, Beaverton, Oregon 97006
Received June 16, 1987; Revised Manuscript Received October 2, 1987

ABSTRACT: Nitric oxide forms adducts with the binuclear iron site of hemerythrin (Hr) at [Fe(II),Fe(II)]deoxy and [Fe(II),Fe(III)]semimet oxidation levels. With deoxyHr our results establish that (i) NO binds reversibly, forming a complex which we label deoxyHrNO, (ii) NO forms a similar but distinct complex in the presence of fluoride, which we label deoxyHrFNO, (iii) NO is directly coordinated to one iron atom of the binuclear pair in these adducts, most likely in a bent end-on fashion, and (iv) the iron atoms in the binuclear sites of both deoxyHrNO and deoxyHrFNO are antiferromagnetically coupled, thereby generating unique electron paramagnetic resonance (EPR) detectable species. The novel EPR signal of deoxyHrNO (deoxyHrFNO) with $g_{\|} = 2.77$ (2.58) and $g_{\perp} = 1.84$ (1.80) is explained by the magnetic interaction of the Fe(II) ($S' = 2$) and $\{FeNO\}^7$ ($S = {}^3/_2$) centers observed by Mössbauer spectroscopy. Antiferromagnetic coupling leads to a ground state of $S^{eff} = {}^1/_2$. Analysis of the EPR parameters using the isotropic spin-exchange Hamiltonian, $\hat{H}_{ex} = 2J\hat{S}_{3/2'}\hat{S}_2$, and including zero-field splitting leads to a coupling constant, $-J \sim 23$ cm^{-1}, for deoxyHrNO. The resonance Raman spectrum of deoxyHrNO shows features at 433 and 421 cm^{-1} that shift downward with $^{15}N^{16}O$ and that are assigned to stretching and bending modes, respectively, of the $\{FeNO\}^7$ unit. Sensitivity of the bending mode to D_2O suggests that bound NO participates in hydrogen bonding. We propose that the terminal oxygen atom of NO is hydrogen bonded to the proton of the μ-hydroxo bridge in the Fe-(OH)-Fe unit. A bent Fe-N-O geometry is supported by spectroscopic and structural comparisons to synthetic complexes and is consistent with a limiting [Fe^{II},$Fe^{III}NO^-$] formulation for deoxyHrNO. Reversibility of NO binding to deoxyHr is demonstrated by bleaching of the optical and EPR spectra of deoxyHrNO upon additions of excess N_3^- or CNO^-. DeoxyHrNO undergoes autoxidation under anaerobic conditions over the course of several hours. The product of this autoxidation appears to be an EPR-silent NO adduct of semimetHr. The formal one-electron oxidations of the binuclear iron site of deoxyHr by NO and by HNO_2 can conceivably occur with no net change in charge on the iron site. In contrast, autoxidation of oxy- to metHr requires a change in net charge on the iron site, which may provide a kinetic barrier.

The non-heme iron oxygen-carrying protein hemerythrin (Hr),[1] which is found in several phyla of marine invertebrates, poses evolutionary, physiological, and biochemical contrasts to the more widespread heme oxygen carriers (Wilkins & Harrington, 1983; Klotz & Kurtz, 1984; Kurtz, 1986). Hemerythrins from erythrocytes of sipunculan worms usually consist of octamers ($M_r \sim 108\,000$) of essentially identical subunits. Each subunit contains a binuclear iron site that reversibly binds one molecule of O_2. The structure of this site in the azide adduct of [Fe^{III},Fe^{III}]metHr (metHrN_3) was determined by X-ray crystallography (Stenkamp et al., 1984; Sieker et al., 1982):

† This research was supported by grants from the National Institutes of Health (D.M.K., GM 37851; P.D., GM 16406; T.M.L. and J.S.-L., GM 18865).
* Address correspondence to this author at the Department of Chemistry, University of Georgia, Athens, GA 30602.

[1] Abbreviations: Hr, hemerythrin; deoxyHr, deoxyhemerythrin; metHr, methemerythrin; deoxyHrNO, NO adduct of deoxyHr; deoxyHrFNO, NO adduct of deoxyHr in the presence of excess fluoride; Tris, tris(hydroxymethyl)aminomethane; EDTA, ethylenediaminetetraacetate; OAc, acetate; $HBpz_3$, tri-1-pyrazolylborate; EPR, electron paramagnetic resonance.

0006-2960/88/0427-1014$01.50/0

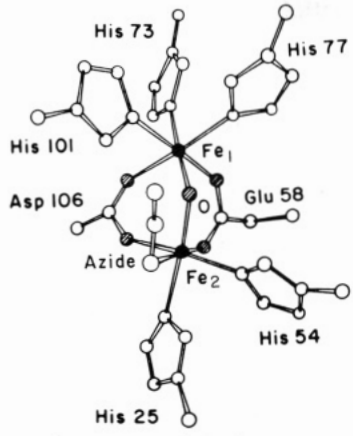

The site has two iron atoms linked to the protein by five terminal imidazole and two bridging carboxylate ligands. A third bridging ligand is provided by the solvent in the form of an oxo ion. The exogenous azide ion is bound to Fe2 in a bent end-on fashion. A number of other small anions (e.g., SCN^-, CN^-) can occupy the same site in the met form of Hr. X-ray crystallography also shows that, in the absence of these anions, the N_3^- binding site is vacant in metHr.

The two forms of the iron site participating in the reversible oxygenation reaction are

$$\underset{\text{deoxy}}{[Fe^{II}(\mu\text{-}OH^-)Fe^{II}]} + O_2 \leftrightarrow \underset{\text{oxy}}{[Fe^{III}(\mu\text{-}O^{2-})Fe^{III}O_2H^-]}$$

The hydroperoxide in oxyHr appears to be bound end-on in a similar orientation to that of azide ion in $metHrN_3$, whereas in deoxyHr once again this exogenous ligand site appears to be vacant (Stenkamp et al., 1985; Shiemke et al., 1984).

The binuclear iron sites in oxy- and metHrs have ground spin states with $S = 0$ due to antiferromagnetic coupling between the iron atoms (Dawson et al., 1972). This coupling is conserved, albeit at lower magnitudes, in both deoxyHr and in an intermediate [Fe(II),Fe(III)] oxidation level referred to as semimetHr. The smaller degrees of antiferromagnetic coupling in anion adducts of semimetHr and in deoxyHr have been attributed to protonation of the μ-oxo bridge with essential retention of the remaining structural features in metHr (Reem & Solomon, 1984, 1987; Maroney et al., 1986; Pearce et al., 1987). In deoxyHr the resulting $S = 0$ ground spin state is EPR-silent. In semimetHr, however, the resulting $S = {}^1/_2$ ground spin state gives rise to an EPR signal with $g_{av} \sim 1.84$ observable below 30 K (Muhoberac et al., 1980). One-electron reduction of metHr yields so-called $(semimet)_RHr$, whereas one-electron oxidation of deoxyHr yields so-called $(semimet)_OHr$. These two forms of semimetHr are distinguishable by the rhombicity of their g tensors and by their redox kinetics [Wilkins and Harrington (1983) and references cited therein].

We have recently examined the oxidation of deoxyHr by nitrite (Nocek et al., 1984) and have also published a preliminary characterization of the NO adduct of deoxyHr (Nocek et al., 1985). We have shown that the unpaired electron on NO turns the iron site of deoxyHr into an EPR-observable center, one in which magnetic coupling between iron atoms is more readily detectable. One reason for undertaking these studies was to examine one-electron oxidations of the iron site in deoxyHr with "inner-sphere" reagents. Previous one-electron oxidations of the iron site have used "outer-sphere" oxidizing agents, such as $[Fe(CN)_6]^{3-}$ [Wilkins and Harrington (1983) and references cited therein]. Reactions of inner-sphere reagents such as NO and HNO_2/NO_2^- would more effectively mimic that of O_2, while presenting the possibility of yielding an isolable product whose iron site may model that of a putative superoxo intermediate, $[Fe^{II},Fe^{III}O_2^-]$, in the oxygenation reaction.

The results presented here describe the chemical and physical characterizations of the reactions of NO with the iron site of Hr in its various oxidation levels.

Experimental Procedures

Isolation and Purification of Hrs. Octameric Hrs from coelomic erythrocytes of three species of sipunculan worms were used in this study. Live worms of the species *Phascolopsis gouldii* were obtained from the Marine Biological Laboratory, Woods Hole, MA. OxyHr was isolated and purified by a standard procedure (Klotz et al., 1957). The crystalline oxyHr was stored frozen in liquid N_2 until used. Live worms of the species *Themiste zostericola* were obtained from Pacific Biomarine Supply, Venice, CA. Live specimens of *Themiste dyscritum* were kindly supplied by Dr. Robert C. Terwilliger of the Oregon Institute of Marine Biology, Charleston, OR. OxyHr from these latter two species was isolated and purified similarly to that from *P. gouldii* except that the crystallization step was omitted. Solutions of *T. dyscritum* Hr were stored at 4 °C. Most of the experimental work was performed on *P. gouldii* Hr. Use of Hr from other organisms is specifically noted in the text.

Preparations of OxyHr and DeoxyHr. Solutions of oxyHr were prepared either by dissolving crystals of oxyHr in buffer, usually 50 mM sodium phosphate, pH 6.5, or by exposing solutions of deoxyHr to air. Concentrations of oxyHr were determined with $\epsilon_{500} = 2200\ M^{-1}\ cm^{-1}$ (Garbett et al., 1969). All concentrations are expressed per binuclear iron sites. For conversion to deoxyHr, solutions of oxyHr were dialyzed anaerobically at 4 °C against 5–15 mM $Na_2S_2O_4$ (BDH Chemicals Ltd., Poole, England) in buffer, usually 50 mM phosphate, pH 6.5. Dialysis was allowed to proceed for at least 12 h in order to ensure complete reduction of the small percentage of the met oxidation level in these solutions. Excess $Na_2S_2O_4$ was then removed by anaerobic dialysis against several changes of buffer. When concentrations of deoxyHr in excess of 2 mM were desired, 0.3 M sodium sulfate was included in all buffers. We have found that sodium sulfate tends to increase the solubility of *P. gouldii* deoxyHr. Solutions of deoxyHr were transferred anaerobically from the dialysis bag into 2-dram vials according to the following procedure. The glass vial was placed in a 50-mL 24/40 Schlenk-type flask attached to a vacuum manifold via the side-arm stopcock. The flask was sealed with a tight-fitting rubber septum and alternately evacuated and flushed with Ar several times. The septum was then removed, and with a steady stream of Ar flowing through the side arm, the dialysis bag containing deoxyHr was cut open and drained into the glass vial. The vial was quickly capped with a tight-fitting rubber septum and then filled with Ar through a hypodermic needle attached to the vacuum manifold. Concentrations of deoxyHr were determined by exposing a sample to air and measuring the optical spectrum of oxyHr.

Preparation of MetHr. MetHr was prepared by addition of a slight molar excess of $K_3Fe(CN)_6$ to solutions of oxyHr. Reaction was allowed to proceed for several hours at room temperature. Excess oxidant was removed by dialysis at 4 °C aainst several changes of buffer, usually 50 mM phosphate, pH 6.5. Concentrations of metHr were determined by addition of excess NaN_3 and use of $\epsilon_{446} = 3700\ M^{-1}\ cm^{-1}$ for $metHrN_3$ (Garbett et al., 1969).

Preparation of $(Semimet)_RHr$ and $(Semimet)_OHr$. These preparations are based on previously described procedures (Babcock et al., 1980). $(Semimet)_RHr$ was prepared by

one-electron reduction of metHr with $Na_2S_2O_4$. Solutions of $(Semimet)_OHr$ were prepared by one-electron oxidation of deoxyHr with $K_3Fe(CN)_6$. After standardization of 50–100 mM solutions of $Na_2S_2O_4$, 1 reducing equiv was injected into an anaerobic solution of 0.5–5 mM metHr, producing $(semimet)_RHr$ within 1–2 min. Similar concentrations of solutions of $K_3Fe(CN)_6$ and deoxyHr were used to produce $(semimet)_OHr$ in 3–5-min reaction time. Because of their tendencies toward slow disproportionation in phosphate buffers, *P. gouldii* $(semimet)_RHr$ and $(semimet)_OHr$ were used or frozen within 5 min of preparation. Solutions of $Na_2S_2O_4$ were standardized by reaction with standard solutions of $K_3Fe(CN)_6$, whose concentrations were determined with $\epsilon_{419} = 1030\ M^{-1}\ cm^{-1}$ (Irwin et al., 1983).

Preparation of DeoxyHrNO. Solutions of deoxyHrNO were prepared by direct addition of gaseous NO either to solutions of deoxyHr or to degassed solutions of oxyHr. Nitric oxide (99.0% minimum purity) was obtained from Matheson Gas Products. This gas was passed through 1.0 M NaOH in order to remove trace impurities of higher oxides of nitrogen. Volumes of gas were withdrawn from above the NaOH solution and injected directly into solutions of deoxyHr via gas-tight syringes. For most preparations, NO was injected in several aliquots with vigorous swirling to anaerobic solutions of 1–2 mM deoxyHr in 50 mM phosphate, pH 6.5. The amount of NO injected was estimated from the ideal gas law. Usually, the mole ratio of NO to Hr was 1.5–5 (0.1–0.33 mL of NO/mL of Hr solution). Use of this procedure at room temperature resulted in complete formation of deoxyHrNO within 5 min.

DeoxyHrNO was also prepared from deaerated solutions of oxyHr in 50 mM phosphate, pH 6.5, or 0.2 M Tris–sulfate, pH 8.0. Prior to injection of NO, the solution of oxyHr was alternately evacuated and flushed with Ar to remove excess dissolved oxygen. This procedure does not completely deoxygenate the Hr. NO gas was then injected as described above. Excess NO gas reacts with the remaining O_2, so that oxyHr is no longer detectable in these preparations.

Preparation of DeoxyHrFNO. DeoxyHrF was prepared by addition of a 1–5 mM solution of deoxyHr in 50 mM phosphate, pH 6.5, to a weighed amount of sodium fluoride to make the resulting solution 0.1–1.0 M in fluoride. After incubation of this solution for ~1 h at room temperature, gaseous NO was injected as described above for preparation of deoxyHrNO. Formation of deoxyHrFNO was complete within 5 min at room temperature as judged by the visible absorption spectrum. DeoxyHrFNO is sufficiently stable so that samples can be concentrated under N_2 with an Amicon ultrafiltration cell equipped with a PM-30 membrane. This method was used to prepare deoxyHrFNO at ~10 mM for Mössbauer spectroscopy.

Preparations of $(Semimet)_RHrNO$ and $(Semimet)_OHrNO$. A two- to tenfold molar excess of gaseous NO was injected via gas-tight syringe directly into anaerobic solutions of 0.1–2.0 mM $(semimet)_OHr$ or $(semimet)_RHr$ in 50 mM phosphate, pH 6.5. Injections of NO and mixing were performed as described above for the preparation of deoxyHrNO. The reactions were complete within 5 min at room temperature as judged by absorption spectra.

Isotopic Enrichment of Samples. ^{15}N-Labeled nitric oxide was prepared by reduction of $Na^{15}NO_2$ (MSD Isotopes, 99 atom% ^{15}N, 91% chemically pure) with L-ascorbate. Typically, 3 mL of a 0.1 M anaerobic solution of L-ascorbic acid in 50 mM phosphate, pH 6.5, was injected into a degassed vial containing ~21 mg of $Na^{15}NO_2$. Nitrite was employed as the limiting reagent, and the amount used was such that the solubility limit of 1.9 mM for NO at 1 atm (Ram & Stanbury, 1984) would be exceeded. The gas above the solution was used without purification immediately after addition of the ascorbate solution in order to keep the production of contaminating gases to a minimum. The labeled gas was added to solutions of deoxyHr and deoxyHrF as described above for unlabeled NO.

^{18}O was incorporated into the μ-oxo bridge of Hr by dissolving crystals of *P. gouldii* deoxyHr in $H_2{}^{18}O$ buffered with 0.2 M Tris–sulfate, pH 8.0. After storage for 2 days in a sealed vial at 4 °C, the solution was exposed to air, causing conversion to oxyHr (Shiemke et al., 1984). A sample in which ^{18}O was present in the bound nitrosyl group, but not in the μ-oxo bridge position of deoxyHrNO, was prepared by dissolving crystalline oxyHr in buffered $H_2{}^{18}O$ and injecting NO within a few hours of dissolution. Under these conditions exchange of the μ-oxo bridge with solvent does not occur to an appreciable extent. The solution had been degassed to remove excess dissolved oxygen prior to addition of NO. However, the trace amounts of O_2 remaining lead to production of NO_2. In aqueous solution NO_2 is known to catalyze exchange of oxygen between NO and H_2O (Bonner, 1970), which in this case results in formation of $^{14}N^{18}O$.

Deuterium substitution into deoxyHrNO was achieved by replacing the solvent H_2O with D_2O prior to addition of nitric oxide. A solution of oxyHr in 50 mM phosphate, pH 6.5, was concentrated and rediluted with buffered D_2O in an Amicon ultrafiltration cell equipped with a PM-30 membrane. This process was repeated 3–4 times until the solvent was greater than 95% D_2O. Gaseous NO was injected into the solution of degassed oxyHr as described above for the preparation of deoxyHrNO. Alternatively, damp crystals of deoxyHr were dissolved into ~8 volumes of phosphate-buffered D_2O containing 0.3 M Na_2SO_4. The solution was incubated for 1 h at room temperature prior to addition of gaseous nitric oxide. No differences in Raman spectra were observed for samples prepared by either method. DeoxyHrFNO in D_2O was prepared similarly from crystalline deoxyHr except that after dissolution of the crystals in D_2O the solution of deoxyHr was allowed to incubate for 20 h prior to addition of fluoride and nitric oxide as described above for the preparation of deoxyHrFNO.

Reactivities of DeoxyHrNO and DeoxyHrFNO. Reactivities were examined by EPR and optical absorption spectroscopies. For EPR spectroscopy 1–2 mM solutions of deoxyHrNO or deoxyHrFNO were prepared in 50 mM phosphate, pH 6.5, containing 0.3 M Na_2SO_4 as described above. After incubation for various times, aliquots were transferred to Ar-filled 4 mm o.d. quartz tubes and frozen in a liquid N_2 bath. The tubes were then evacuated, flame-sealed, and stored at liquid N_2 temperature. For monitoring by optical absorption spectroscopy, 0.1–1.0 mM samples of Hr were used. Both optical and EPR spectra were obtained up to 24 h after preparation. A 10-fold or greater molar excess of NaN_3 was added to the final samples, and spectra of the resulting products were recorded.

Reactions with O_2 were examined by bubbling air through solutions of the NO adducts for 1–3 min prior to recording optical spectra. Reactions with N_3^-, CNO^-, F^-, Cl^-, Br^-, I^-, SCN^-, and CN^- were examined by injection of aliquots of freshly prepared buffered solutions of the NO adducts of Hr into measured amounts of the sodium salts of each anion. The final concentrations of anions were 0.1, 0.5, or 1.0 M. Optical and EPR spectra were obtained immediately after mixing and

after ~30-min incubation at room temperature.

Physical Measurements. Optical spectra were obtained on a Perkin-Elmer Model 554 dual-beam spectrophotometer. Quartz cells of 1-cm path length were used. For air-sensitive samples, the cell was equipped with a side arm containing a Teflon stopcock. One-milliliter samples were injected under Ar via gas-tight syringe through double-septum seals (Averill et al., 1978).

EPR spectra were obtained on a Bruker Model ER-220D spectrometer operating at X-band and equipped with an Oxford Instruments ESR-10 liquid helium flow system. Sample volumes were typically 100–200 μL and were prepared as described above under Reactivities of DeoxyHrNO and DeoxyHrFNO. Unless otherwise stated, spectral conditions were as follows: temperature, 4.5 ± 0.5 K; frequency, 9.5 ± 0.1 GHz; modulation amplitude, 16 or 40 G at 100 kHz; microwave power, 100 μW; scan time, 200 s; time constant, 0.1–0.2 s. EPR power saturation data were collected by measuring the EPR absorption derivative signal intensity, I, as a function of incident microwave power, P. Data were analyzed according to

$$\log (I/\sqrt{P}) = a - (b/2) \log (P_{1/2} + P)$$

and the half-saturation power, $P_{1/2}$, was determined by a graphical method (Yim et al., 1982). Spin quantitations were achieved by double integrations of first-derivative EPR spectra obtained under nonsaturating conditions. The resulting areas were compared to those obtained from copper sulfate standards of similar concentrations, whose spectra were recorded with indentical instrument settings (Wertz & Bolton, 1972; Aasa & Vanngard, 1975).

^{57}Fe Mössbauer spectra were collected in the Department of Physics at the Univesity of Illinois. The spectrometer was of the constant-acceleration type. Samples contained the natural isotopic abundance of ^{57}Fe. Isomer shifts are quoted relative to iron metal at 300 K. The data accumulated at 100 K were fitted with a sum of Lorentzians by a least-squares routine (Chrisman & Tumolillo, 1971). A sample of deoxyHrFNO (~10 mM solution) was prepared as described above, and ~1 mL of this sample was transferred anaerobically via gas-tight syringe to a cylindrical nylon cup 0.5 in. in diameter. The sample was then frozen immediately in a liquid N_2 bath.

Resonance Raman spectra were obtained at the Oregon Graduate Center, Beaverton, OR, on a computer-interfaced Jarrell-Ash spectrophotometer. A Spectra-Physics 164-01 Kr^+ laser was used to produce an excitation frequency of 647.1 nm. The scattered light was detected on an RCA C31034 photomultiplier tube and processed in an ORTEC Model 9302 amplifier/discriminator. A backscattering geometry of 150° was used. Spectra were collected at 90 K unless otherwise noted. In order to maintain this temperature, samples were kept in a liquid N_2 coldfinger having a transparent window (Sjöberg et al., 1982). The incident light (70–120 mW) was focused upon samples (~20 μL) contained in open-ended capillary tubes [(1.5–1.8) × 90 mm] sealed with either Apiezon-N or Dow Corning sealant. Further spectral parameters are given in the table and figure legends. All samples were examined prior to Raman spectroscopy to ascertain the presence of either the deoxyHrNO or deoxyHrFNO EPR signal.

Results

Preparations of DeoxyHrNO and DeoxyHrFNO. Gradual addition of a 1.5–5-fold molar excess of gaseous nitric oxide to an anaerobic solution of either oxy- or deoxyHr results in formation of a pine green adduct, which we refer to as deoxyHrNO. The cleanest preparations of deoxyHrNO are obtained below pH 7.5. In the presence of ≳50-fold molar excess of fluoride over deoxyHr, addition of NO as described above results in formation of an adduct with properties similar to but distinct from those of deoxyHrNO. We refer to the NO adduct of deoxyHr in the presence of this large excess of fluoride as deoxyHrFNO. The properties of these adducts do not change significantly between pH 6.5 and pH 8.5, but the adducts become unstable at pH 10.

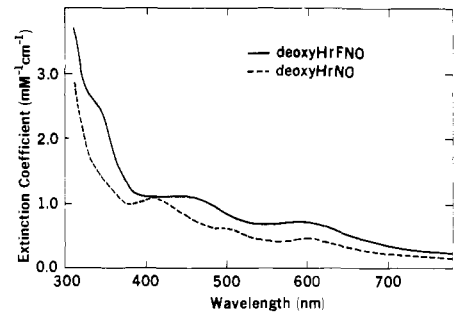

FIGURE 1: Optical spectra of deoxyHrNO (dashed curve) and deoxyHrFNO (solid curve) in 50 mM phosphate, pH 6.5, under anaerobic conditions.

Table I: Spectral Properties of *P. gouldii* DeoxyHrNO and DeoxyHrFNO

parameter	deoxyHrNO	deoxyHrFNO
	Optical	
λ (nm) (ε [M^{-1} cm^{-1}])		340 sh (2700)
	408 (1200)	450 (1200)
	500 sh (700)	
	600 (500)	590 (750)
	EPR at 4 K	
$g_\parallel$	2.77 ± 0.02	2.58 ± 0.01
$g_\perp$	1.84 ± 0.02	1.80 ± 0.02
$P_{1/2}$ (mW)	0.060	12
	Mössbauer at 100 K	
$\delta_{Fe}(\Delta E_Q)$ (mm/s)		
$S = {}^3/_2$, {FeNO}^{7}	0.68 (0.61)	0.75 (1.02)
$S = 2$, Fe(II)	1.21 (2.65)	1.22 (3.09)
	Resonance Raman at 90 K	
ν(Fe–N) (cm^{-1})	433	420
δ(Fe–N–O) (cm^{-1})	421	not observed

Optical Absorption Spectra. The optical spectra and extinction coefficients for these two derivatives are given in Figure 1 and Table I. The optical spectrum of deoxyHrNO contains peaks at 600, 500, and 408 nm. These compare with the broader peaks at 590 and 450 nm in the spectrum of deoxyHrFNO, which, in addition, contains a relatively intense shoulder at 340 nm.

EPR Spectra. Figure 2 shows the X-band EPR spectra of deoxyHrNO and deoxyHrFNO from *P. gouldii* at 4 K. Both adducts exhibit broad, axial signals, whose g values (Table I) are similar to, but distinct from, each other.[2] *T. dyscritum* deoxyHrNO, prepared from either oxy- or deoxyHr, exhibits an EPR spectrum with $g_\parallel = 2.68$ and $g_\perp = 1.89$ very similar to that shown in Figure 2A for *P. gouldii* deoxyHrNO.

[2] At low microwave powers (≲80 μW), the EPR spectrum of deoxyHrFNO (and occasionally the spectrum of deoxyHrNO) contains a sharp radical signal at $g = 2.03$ (Figure 2B). At higher microwave powers, this radical signal disappears (Figure 2C). Both the sharpness of this signal and its relative ease of saturation suggest that it is not a metal-derived signal.

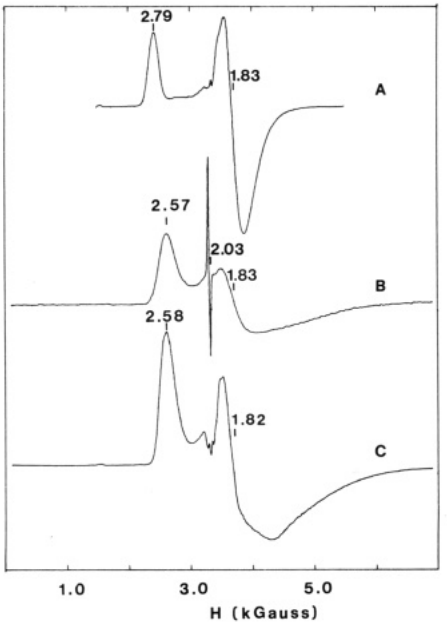

FIGURE 2: EPR spectra at 4 K of (A) deoxyHrNO at 40 μW and gain of 5×10^4, (B) deoxyHrFNO at 40 μW and gain of 8×10^4, and (C) deoxyHrFNO at 6.3 mW and gain of 8×10^3. Other spectral conditions are given under Experimental Procedures. Concentrations are as follows: (A) 1.4 mM Hr, [NO]/[Hr] = 1.4; (B) 3.1 mM Hr, 142 mM NaF, [NO]/[Hr] = 9.5; (C) 3.25 mM Hr, 644 mM NaF, [NO]/[Hr] = 4.6. Buffer is 50 mM phosphate, pH 6.5.

Double integrations of the *P. gouldii* deoxyHrNO EPR signal, obtained at 4.2 K from seven independently prepared samples, against a copper sulfate standard yielded 0.91 ± 0.07 spin/2 Fe. Thus, conversion to the EPR active center is essentially quantitative. The value of the half-saturation power, $P_{1/2}$, at 4.2 K for the deoxyHrFNO EPR spectrum was determined to be ~12 mW, compared to ~60 μW for deoxyHrNO. Double integrations of the deoxyHrFNO EPR signal never accounted for more than 50% of the binuclear iron sites. While this signal is much broader than the copper sulfate concentration standard, we are unable to account for a discrepancy of this magnitude. The Mössbauer spectra of deoxyHrFNO (vide infra) indicate the presence of a 7% impurity of the fluoride adduct of metHr (metHrF) but suggest that the sample is otherwise homogeneous.

For relaxation by an Orbach process, the EPR half-saturation power $P_{1/2}$, as a function of absolute temperature T, has been well fitted in other systems (Yim et al., 1982; Rutter et al., 1984; Pearce et al., 1987a) at all but the lowest temperatures by

$$\ln P_{1/2} = \ln A - \Delta/kT$$

where k is the Boltzmann constant and A is a constant characteristic of the particular system. The value of Δ is a measure of the energy separation between the ground state and the first excited state. A plot of $\ln P_{1/2}$ (in mW) vs $1/T$ for the $g_\perp$ component of the deoxyHrNO EPR spectrum is shown in Figure 3. Least-squares analysis of the linear portion of this plot generated the slope, Δ/k, of the line shown in Figure 3. The value of Δ determined from this plot is 72 cm^{-1}. The analogous plot (not shown) fo the $g_\parallel$ component yielded $\Delta = 68$ cm^{-1}. Because the required microwave powers exceeded those available on our spectrometer, we were unable to obtain values of $P_{1/2}$ for the deoxyHrFNO EPR signal at temperatures much higher than 4.2 K.

Mössbauer Spectra. The ^{57}Fe Mössbauer spectrum of deoxyHrNO at 100 K consists of a pair of doublets of approximately equal intensities having the isomer shifts, δ_{Fe}, and quadrupole splittings, ΔE_Q, listed in Table I (Nocek et al., 1985). The Mössbauer spectrum of deoxyHrFNO at 100 K is shown in the upper spectrum of Figure 4 together with Lorentzian fits. The lower spectra of Figure 4 is of the same sample at 4.2 K.[3] Analogously to the spectrum of deox-

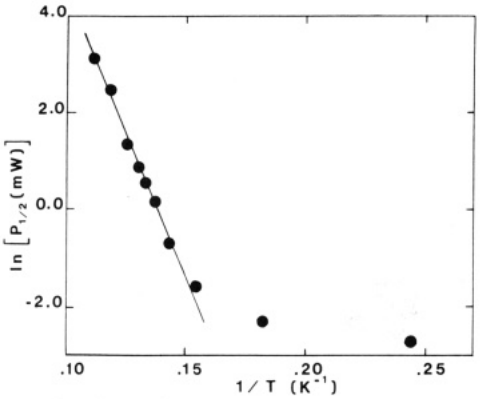

FIGURE 3: Dependence of the EPR half-saturation power, $P_{1/2}$, on absolute temperature for deoxyHrNO. [Hr] = 4.6 mM; [NO]/[Hr] = 5. Buffer is 50 mM phosphate, pH 6.5, with 0.3 M sodium sulfate. Normalized peak-to-trough intensities of the $g = 1.84$ feature were used to determine $P_{1/2}$ at each temperature as described under Experimental Procedures.

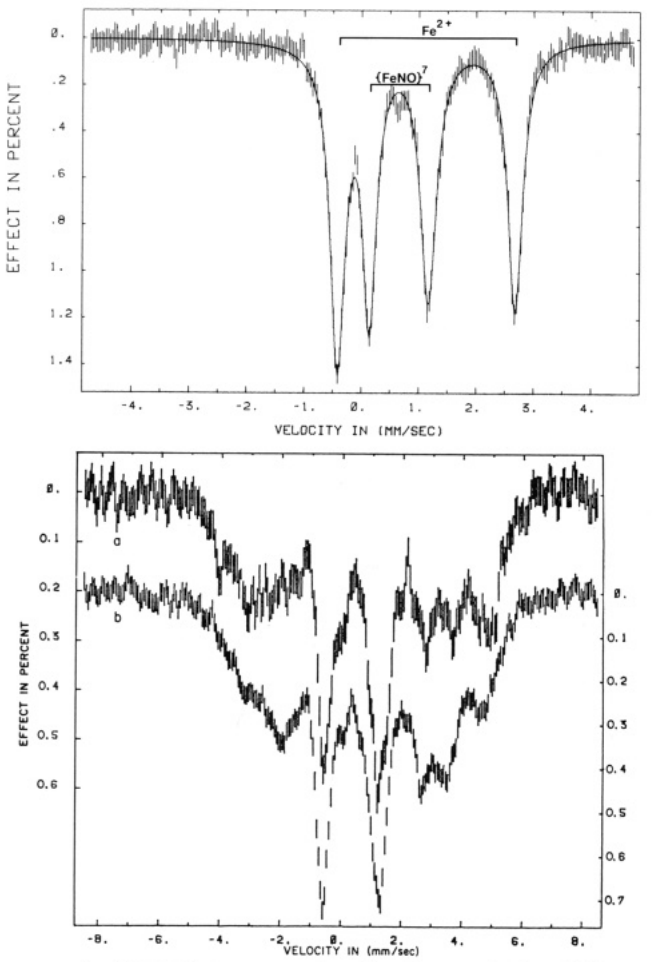

FIGURE 4: ^{57}Fe Mössbauer spectra of a frozen solution of deoxyHrFNO at 100 K in zero applied field (upper spectrum) and 4.2 K in a field of 0.22 T (lower spectra) applied parallel (a) and perpendicular (b) to the direction of the γ-ray beam. The solid curve in the upper spectrum represents a Lorentzian fit with the parameters listed in Table I. [Hr] = 9.8 mM, [F$^-$] = 644 mM, and [NO]/[Hr] = 4.6. Buffer is 50 mM phosphate, pH 6.5.

Table II: Resonance Raman Isotope Shifts and Relative Intensities for *P. gouldii* DeoxyHrNO[a]

isotopic composition	ν(Fe–N) (cm^{-1})	δ(Fe–N–O) (cm^{-1})	I for δ(Fe–N–O)/I for ν(Fe–N)
$^{14}N^{16}O$	433	421	0.30
$^{15}N^{16}O$	426	415	0.38
$^{14}N^{18}O$[b]	427	414	0.21
$^{14}N^{16}O$ in D_2O	432	414	0.17

[a] Peak positions and relative intensities determined by curve-fitting with 90% Lorentzian–10% Gaussian product functions having a full width at half-height of 18 cm^{-1} for H_2O samples and 14 cm^{-1} for D_2O samples. Spectral conditions as in Figure 5. [b] Sample with Fe–^{18}O–Fe in $H_2{}^{18}O$.

yHrNO, we pair the outermost and innermost lines in the upper spectrum of Figure 4, which yields two quadrupole doublets with parameters as listed in Table I. Our previously published Mössbauer spectrum at 100 K of deoxyHrNO shows approximately equal intensities of inner and outer doublets (Nocek et al., 1985). Apart from a 7% impurity,[3] the upper spectrum of Figure 4 is compatible with the presence of equal amounts of two and only two distinct iron centers. We also reported previously that both doublets in the Mössbauer spectrum of deoxyHrNO broaden at 4.2 K (Sage & Debrunner, 1986). Figure 4B shows that such broadening occurs in the spectrum of deoxyHrFNO as well. The broadenings of the inner and outer doublets in the 4.2 K spectra of both deoxyHrNO and deoxyHrFNO confirm that both iron centers in each adduct are associated with the corresponding paramagnetic center indicated by EPR. The Mössbauer spectrum of deoxyHr does not show significant broadening under the conditions of the lower spectrum in Figure 4 (Garbett et al., 1971).

The parameters of the outer doublets in the 100 K spectra of both deoxyHrNO and deoxyHrFNO are similar to, but not identical with, published values for the single doublet of *P. gouldii* deoxyHr at 77 K, namely, $\delta_{Fe}(\Delta E_Q)$ 1.19 (2.81) mm/s (Okamura et al., 1969; Garbett et al., 1971). Thus, this outer doublet is logically assigned to a high-spin Fe(II) center. The parameters of the inner pairs of lines in the spectra of deoxyHrNO and deoxyHrFNO (Table I) fall near the ranges of $\delta_{Fe}(\Delta E_Q)$, 0.6–0.7 (0.6–1.7) mm/s, observed for $\{FeNO\}^7$ $S = {}^3/_2$ centers of the type that do not undergo spin crossover (Arciero et al., 1983; Wells et al., 1982; Hodges et al., 1979; Bill et al., 1985).[4] The $\{FeNO\}^7$ notation follows that of Enemark and Feltham (1974) for ferrous nitrosyls. In light of the Mössbauer results, the EPR spectra of deoxyHrNO and deoxyHrFNO are logically interpreted as arising from antiferromagnetic coupling of an Fe(II) $S = 2$ with an $\{FeNO\}^7$ $S = {}^3/_2$ giving a ground state with $S^{eff} = {}^1/_2$ (Nocek et al., 1985).

Resonance Raman Spectra. Resonance Raman spectra of deoxyHrNO obtained at 90 K with 647.1-nm excitation are shown in Figure 5. Shorter excitation wavelengths produced a large fluorescence background that prevented observation of any Raman bands. Raman bands due to the internal NO vibration were searched for intensively in the 1400–1900-cm^{-1} region but were not detected. Raman features due to the FeNO moiety were, however, observed at lower energy. The spectrum in Figure 5A, which was obtained with the natural isotopic abundance of NO, shows a broad band centered at 433 cm^{-1}. The 25-cm^{-1} width at half-height and its asymmetry suggest that this band has more than one component. Curve fitting analysis indicates two components at 421 and 433 cm^{-1} in a ~1:3 intensity ratio (Table II). Spectra B and C of Figure 5 display the effects of isotopic substitution of NO on the spectra. Downward shifts in both component bands are observed when either $^{15}N^{16}O$ or $^{14}N^{18}O$ is used in place of $^{14}N^{16}O$, proving that both component bands are due to vibrational modes involving NO. The results of curve-fitting analyses of these latter spectra are listed in Table II. Figure 5D shows that the two component bands are affected differently by D_2O. The 421-cm^{-1} component shifts downward by 7 cm^{-1}, while the 433-cm^{-1} component undergoes at most a shift of −1 cm^{-1}. The more intense band at 433 cm^{-1} is assigned to the Fe–N stretch, with the 421-cm^{-1} shoulder more likely being due to an Fe–N–O deformation. The greater deuterium isotope sensitivity of δ(Fe–N–O) is consistent with the terminal oxygen of the bound NO being involved in hydrogen bonding. If this oxygen were protonated, then ν(Fe–N)

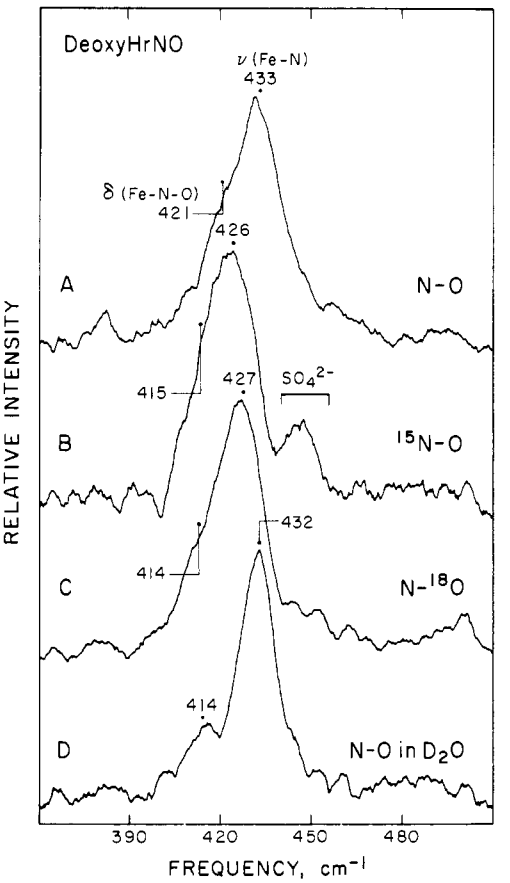

FIGURE 5: Resonance Raman spectra of deoxyHrNO prepared with (A) $^{14}N^{16}O$, (B) $^{15}N^{16}O$, (C) $^{14}N^{18}O$ in $H_2{}^{18}O$, μ-^{18}O-bridged, and (D) $^{14}N^{16}O$ in D_2O. Samples contained 2–8 mM Hr in 50 mM phosphate, pH 6.5, except for the samples in $H_2{}^{18}O$, which were in 0.2 M Tris–sulfate, pH 8.0. All samples contained ~0.3 M Na_2SO_4. Spectra were obtained at 90 K with 647.1-nm excitation (80 mW), 8-cm^{-1} resolution, and 2 cm^{-1}/s scan rate and represent the accumulation of ~25 scans subjected to a Savitsky–Golay smoothing routine.

[3] The two relatively sharp peaks near −0.4 mm/s and +1.3 mm/s in the 4.2 K spectra coincide with lines 1 and 3, respectively, of the 100 K spectrum. This coincidence and the unequal fractional areas (0.29, 0.22, 0.25, 0.24) of the unconstrained Lorentzian fit (solid line in upper spectrum of Figure 4) suggest the presence of an impurity doublet due to a diamagnetic metHr species. After subtraction of a metHrF doublet (Garbett et al., 1969) amounting to 7% of the original area, the four Lorentzians have fractional areas of 0.266, 0.243, 0.229, 0.258, which are pairwise equal within the uncertainty of ±0.007.

[4] We have found $\delta_{Fe}(\Delta E_Q)$ = 0.62 (1.31) mm/s at 4.2 K for [Fe($C_9H_{21}N_3$)(NO)(N_3)$_2$], which has been shown by Pohl et al. (1987) to be the first structurally characterized example of an octahedral $\{FeNO\}^7$ $S = {}^3/_2$ complex. We thank Prof. K. Wieghardt for providing a sample of this complex.

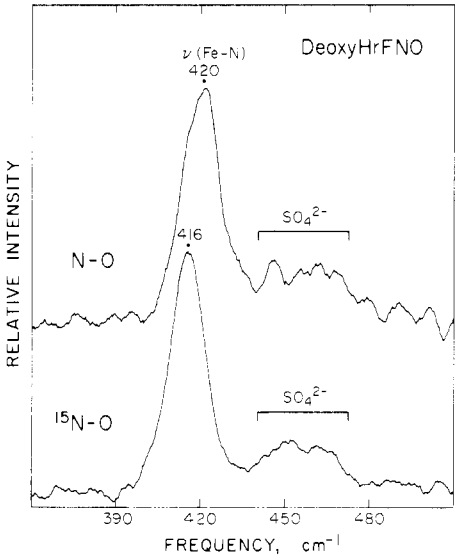

FIGURE 6: Resonance Raman spectra of deoxyHrFNO prepared with $^{14}N^{16}O$ (upper spectrum) and $^{15}N^{16}O$ (lower spectrum). Samples contained ~2 mM Hr in 50 mM phosphate, pH 6.5, with ~0.3 M Na_2SO_4. Spectral conditions as in Figure 5.

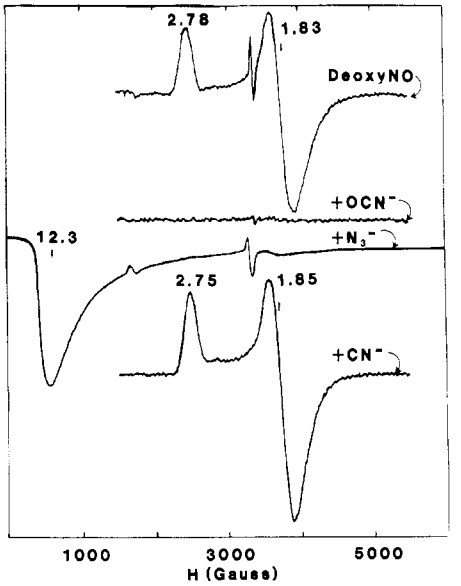

FIGURE 7: EPR spectra of (top) deoxyHrNO and (in descending order) its reaction products with 490 mM CNO^-, 590 mM N_3^-, and 500 mM CN^-. Spectral parameters are as given under Experimental Procedures except that the power is 40 μW in the deoxyHrNO, deoxyHrNO + CNO^-, and deoxyHrNO + CN^- spectra and 100 μW for the deoxyHrNO + N_3^- spectrum. All other parameters were identical for all spectra. Separate samples of the solution of deoxyHrNO giving the top spectrum were used for additions of each anion. [Hr] = 2.1 mM; [NO]/[Hr] = 3.1. Buffer is 50 mM phosphate, pH 6.5.

should have exhibited a significant deuterium dependence as well. The lowered intensity of the δ(Fe–N–O) peak relative to the ν(Fe–N) peak in D_2O is also indicative of hydrogen bonding (Mino et al., 1987).

The resonance Raman spectrum of deoxyHrFNO (Figure 6) shows a single symmetric band at 420 cm^{-1}, which shifts to 416 cm^{-1} with $^{15}N^{16}O$ and which does not shift in D_2O. This mode appears to be analogous to the Fe–N stretch at 433 cm^{-1} in deoxyHrNO but occurs at somewhat lower energy. There was no indication of a resonance-enhanced shoulder attributable to the Fe–N–O deformation in either H_2O or D_2O. Here again, the 1400–1900-cm^{-1} region did not reveal any Raman bands that could be ascribed to ν(N–O).

An alternative explanation for the observation of two NO-dependent vibrations in deoxyHrNO compared to only one in deoxyHrFNO would be the occurrence of multiple protein conformations in deoxyHrNO. For example, hydroxomethemerythrin exhibits two ν_s(Fe–O–Fe) modes due to hydrogen-bonded and non-hydrogen-bonded conformers of the bridging oxo group (Shiemke et al., 1986). When such weak hydrogen bonds are involved, the distribution of species can be altered by varying the temperature. To test this possibility for deoxyHrNO, relative intensities of the two Raman component bands were examined as a function of temperature. This experiment was performed on the deuterium-treated protein, since that spectrum (Figure 5D) provides the clearest resolution of the two Raman bands. No significant change in the relative intensities of the two peaks was observed between 90 and 250 K, indicating that the two vibrational modes are not due to conformers with different degrees of hydrogen bonding. We also investigated the resonance Raman spectra of deoxyHrNO and deoxyHrFNO from a different organism, *T. zostericola*. These spectra exhibited nearly identical peak frequencies and relative intensities compared to those of *P. gouldii* (Figure 5, Table I). In this case, the deoxyHrNO bands were at 433 and 423 cm^{-1} while the deoxyHrFNO band was again at 420 cm^{-1}. Since it is unlikely that such a similar distribution of conformations would occur with proteins from different organisms, we conclude that the two Raman bands are not the result of alternative conformations.

One other possible explanation for the two bands in deoxyHrNO is that they are due to modes involving the μ-hydroxo bridge between the iron atoms. To rule out this alternative, samples of deoxyHrNO were prepared from μ-^{18}O-bridged and μ-^{16}O-bridged oxyHr. The μ-^{16}O-bridged sample was found to exhibit Raman bands at the same frequencies as the μ-^{18}O-bridged sample shown in Figure 5C. These experiments were performed in $H_2{}^{18}O$ solvent, which resulted in isotopic substitution of the added NO. Consequently, it was necessary to ascertain that the ^{16}O-bridged oxyHr sample did not incorporate ^{18}O into the bridging position during or subsequent to formation of deoxyHrNO. Therefore, a portion of this deoxyHrNO sample was oxidized to metHr with $K_3Fe(CN)_6$ and then converted to metHrN_3. The resonance Raman spectrum of the resulting species contained a band at 508 cm^{-1} which is characteristic of the symmetric Fe–O–Fe stretching mode with ^{16}O in the bridging position (Shiemke et al., 1984). If the bridge had exchanged with ^{18}O, this vibration would have occurred at 494 cm^{-1}. Our failure to observe any Raman contribution from the μ-hydroxo bridge is not surprising, since this type of structure has not yielded resonance-enhanced modes either in semimetHrN_3 (Irwin et al., 1983) or in the μ-hydroxo-bridged $[Fe_2OH(Ac)_2(HBpz_3)_2]^+$ complex (Spool, 1985).

Reactivities of DeoxyHrNO and DeoxyHrFNO. The deoxyHrNO complex behaves as expected for a reversible adduct between deoxyHr and NO toward agents such as O_2 or N_3^- which are capable of displacing NO. When O_2 is bubbled through a solution of deoxyHrNO, an ~90% yield of oxyHr is obtained within a few minutes, on the basis of quantitation of the optical spectrum. DeoxyHrFNO is much more slowly reacting with O_2 and undergoes a gradual change in its absorption spectrum over the course of several hours of exposure to O_2. The ultimate product in this case appears to be metHrF, which is consistent with the known ability of F^- to accelerate the autoxidation of oxyHr (Bradić et al., 1977).

We previously reported that addition of excess N_3^- or CNO^- to solutions of deoxyHrNO results in immediate bleaching of the optical spectrum (Nocek et al., 1985). Figure 7 shows that

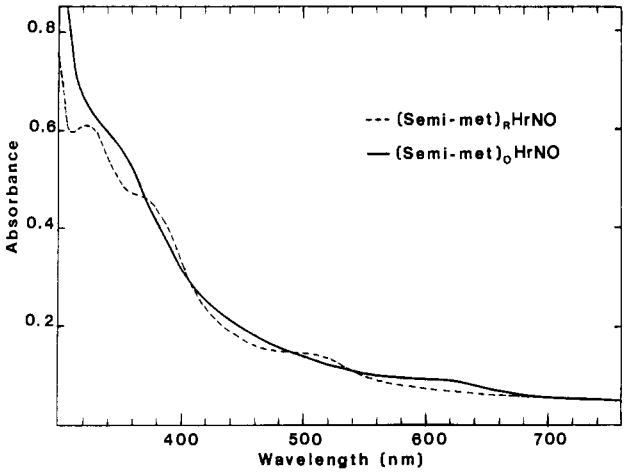

FIGURE 8: Optical spectra of (semimet)$_O$HrNO and (semimet)$_R$HrNO: 0.125 mM Hr in 50 mM phosphate, pH 6.5. [NO]/[Hr] = 8.5 for (semimet)$_O$Hr and 4.6 for (semimet)$_R$Hr. The solution of (semimet)$_O$HrNO contains 0.3 M Na_2SO_4.

the EPR signal vanishes concomitant with this bleaching. Cyanide, on the other hand, has no detectable effect on the EPR signal. In the case of N_3^- addition, the deoxyHrNO EPR signal is replaced by a feature at $g \sim 12$. This latter signal has previously been identified as due to deoxyHrN_3 (Reem & Solomon, 1984). Our results are consistent with the known ability of N_3^- and CNO^- to form complexes with deoxyHr (Reem & Solomon, 1987; Wilkins & Wilkins, 1987). In contrast, anions such as CN^-, Cl^-, Br^-, I^-, and SCN^-, which do not form detectable complexes with deoxyHr, also have no effect on the optical and EPR spectra of deoxyHrNO, when added in a ~200-fold molar excess. An example of this lack of effect is shown for CN^- addition in Figure 7. Addition of excess F^- to deoxyHrNO causes partial conversion to deoxyHrFNO.

Upon anaerobic incubation at room temperature, the EPR signal of deoxyHrNO gradually diminishes; about 40% of the original integrated intensity remains after 6 h. No new signals become visible during this incubation. After 20 h of anaerobic incubation, only 9% of the original integrated EPR intensity remains. Upon addition of NaN_3, the protein at this point was shown to be at the semimet oxidation level by observation of the characteristic semimetHrN_3 EPR signal with g values of 1.91, 1.83, and 1.52 (Muhoberac et al., 1980). In contrast, no changes are observed in spectra of deoxyHrFNO even after 24-h anaerobic incubation at room temperature.

Preparation and Characterization of (Semimet)$_R$HrNO and (Semimet)$_O$HrNO. Addition of a 1–10-fold molar excess of gaseous NO to anaerobic solutions of *P. gouldii* (semimet)$_R$Hr or (semimet)$_O$Hr produce brown adducts, which we refer to as (semimet)$_R$HrNO and (semimet)$_O$HrNO, respectively. In 50 mM phosphate, pH 6.5, the best preparations are obtained when the NO is added within 5 min of preparation of (semimet)$_R$Hr and (semimet)$_O$Hr.

Differences in the optical spectra (Figure 8) indicate that (semimet)$_R$HrNO is not identical with (semimet)$_O$HrNO. The optical spectrum of (semimet)$_R$HrNO has distinct features at λ_{max} (nm) (ϵ[M^{-1} cm^{-1}]) 330 (5000), 380 sh (3500), and 510 (1200). We have shown previously that (semimet)$_R$HrNO is EPR-silent but has the reactivity of a species at the semimet oxidation level, since addition of excess N_3^- generates the EPR spectrum of semimetHrN_3 (Nocek et al., 1984). The (semimet)$_O$HrNO species also appears to be EPR silent, since the EPR spectrum of (semimet)$_O$Hr disappears within 2 min after addition of NO. There is no evidence of any deoxyHrNO EPR signal, such as would occur if (semimet)$_O$Hr were being reduced to deoxyHr by NO. Oxidation to metHr is likewise ruled out since the (semimet)$_O$HrNO optical spectrum of Figure 8 is much different from that of metHr (Garbett et al., 1969), and we have observed no reaction between metHr and up to a 10-fold molar excess of NO. At the concentrations required for either Mössbauer or resonance Raman spectroscopy, we have been unable to obtain homogeneous samples of either (semimet)$_R$HrNO or (semimet)$_O$HrNO.

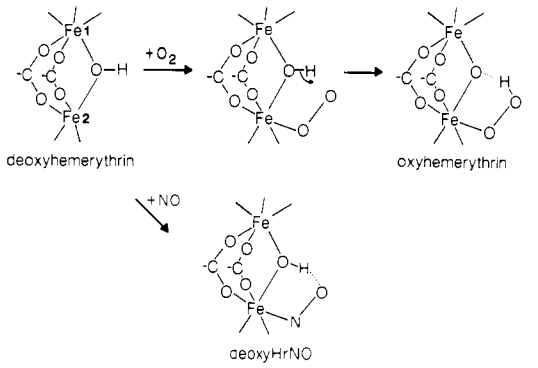

FIGURE 9: Proposed mechanism for reversible oxygenation of Hr [from Stenkamp et al. (1985)] and proposed structure for the binuclear iron site in deoxyHrNO.

Discussion

Reversibility of NO binding to deoxyHr is demonstrated by its conversion to oxyHr on exposure to O_2, by the bleaching of its optical spectrum, and by the disappearance of the EPR signal upon addition of excess N_3^- or OCN^-. Addition of excess F^- leads to partial conversion to deoxyHrFNO. These three anions (and only these three) have previously been shown to form complexes with deoxyHr (Reem & Solomon, 1984, 1987; Maroney et al., 1986; Wilkins & Wilkins, 1987). Other anions are without effect on the optical and EPR spectra of deoxyHrNO.

The reversible binding of dioxygen appears to occur at a vacant iron coordination site in deoxyHr (Figure 9). It is likely that other exogenous ligands such as NO, N_3^-, and CNO^- are bound in this same location. For both deoxyHrNO and deoxyHrFNO, the observation of FeNO vibrational modes by resonance Raman spectroscopy provides clear evidence that the NO is directly bonded to iron in these adducts. Furthermore, the Mössbauer data for the two NO adducts indicate that the NO binds to only one of the iron atoms in the binuclear iron site. Since the structural constraints provided by the surrounding protein favor a severely bent Fe–X–X geometry (X = N, O) for azide and hydroperoxide (Stenkamp et al., 1984, 1985), the NO adducts of deoxyHr are also likely to be bound in a bent, end-on fashion (Figure 9). Although iron coordination of N_3^-, CNO^-, and F^- to deoxyHr is presumed from their spectroscopic perturbations (Reem & Solomon, 1987; Maroney et al., 1986), direct evidence from techniques such as Raman or Mössbauer spectroscopy is still lacking in these cases. This distinction is relevant to the location of F^- in deoxyHrFNO. The significant perturbations of the electronic, EPR, Mössbauer, and Raman spectroscopic properties of deoxyHrNO when this adduct is formed in the presence of fluoride are consistent with simultaneous binding of NO and F^- to the iron site. While the EPR and Mössbauer spectra indicate that an exogenous bridging ligand is retained in deoxyHrFNO, it seems unlikely that the protein would have enough flexibility to accommodate a seven-coordinate species. A more probable structure would be one in which a μ-fluoro bridge replaces the μ-hydroxo bridge between the iron atoms.

Alternatively, fluoride ion could be behaving as an allosteric effector, binding to another part of the protein and altering the conformation at the binuclear site.

The unusual EPR spectrum of deoxyHrNO can be explained by assuming antiferromagnetic coupling of the Fe(II) ($S' = 2$) and {FeNO}^{7} ($S = {}^3/_2$) centers observed by Mössbauer spectroscopy (Nocek et al., 1985). However, as the following arguments show (Sage & Debrunner, 1986), an isotropic exchange interaction between the two spins, $\hat{H}_{ex} = -2J\hat{S}_{3/2}\cdot\hat{S}_2$, is by itself not sufficient to explain the data.

For $-J > 0$, the eigenstates of $\hat{H}_{ex}$ are a ground doublet, a quartet at an energy $\Delta = -3J$, a sextet at $-5J$, etc. The model relates the g tensor of the ground doublet, $g_{1/2}$, to the intrinsic g tensors of the $S = 2$ and $S = {}^3/_2$ centers, g_2 and $g_{3/2}$, respectively, by $g_{1/2} = 2g_2 - g_{3/2}$. Inserting the measured g values and adopting the isotropic value of $g_{3/2} = 2$ found in other Fe(II)NO complexes (Arciero et al., 1983; Bill et al., 1985), we find that the model implies $g_2 = (1.92, 1.92, 2.38)$ and $(1.90, 1.90, 2.29)$ for deoxyHrNO and deoxyHrFNO, respectively. A g value as low as 1.92 is unreasonable for a high-spin ferrous ion, and we therefore conclude that the model is inadequate. If we identify Δ ($=-3J$) with the excited-state energy of ~ 70 cm^{-1} deduced from EPR power saturation measurements (Gayda et al., 1976; Rutter et al., 1983), we obtain an estimate of $-J \sim 23$ cm^{-1} for deoxyHrNO. The exchange interaction is thus not much larger than the zero-field splitting expected for the two spins, $\hat{H}_{zfs} = \sum[D_i(\hat{S}_{iz} - \hat{S}_i(\hat{S}_i - 1)/3) + E_i(\hat{S}_{ix} - \hat{S}_{iy})]$ with the estimated values $|D_2| < 15$ cm^{-1} (Reem & Solomon, 1987) and $D_{3/2} > 10$ cm^{-1} and $E_{3/2} \ll D_{3/2}$ (Arciero et al., 1983). We therefore expect the combined Hamiltonian $\hat{H} = \hat{H}_{ex} + \hat{H}_{zfs}$ to yield a better approximation of the coupled spin system. We have evaluated the eigenstates of this Hamiltonian and have searched for reasonable parameters J, D_2, $D_{3/2}$, and g_2 that approximate the measured values of g^{eff} and Δ. [In order to reduce the number of adjustable parameters to four, we set $E_i = 0$ and use the relation $g_{2x} = g_{2y} = g_{2z} - 2kD_2/\lambda$, $\lambda/k = -125$ cm^{-1}, which follows from the second-order spin Hamiltonian with $E_2 = 0$. See, e.g., eq 19–32 in Abragam and Bleaney (1970).] With inclusion of zero-field splitting, the quartet now splits into two doublets with energies Δ_1 and Δ_2. With the input of parameters $J = -22.5$ cm^{-1}, $D_2 = -6.9$ cm^{-1}, $D_{3/2} = -18$ cm^{-1}, and $\langle g_2\rangle = 2.18$, we find $\Delta_1 = 67.5$ cm^{-1}, $\Delta_2 = 85.0$ cm^{-1}, and a g tensor $g_{1/2} = (1.85, 1.85, 2.76)$. The calculated values of Δ_1 and $g_{1/2}$ are very close to those measured for deoxyHrNO. While unlikely to be unique, this solution demonstrates that, using reasonable values of J, D_2, $D_{3/2}$, and $\langle g_2\rangle$, the observed EPR parameters of deoxyHrNO can be satisfactorily described in terms of antiferromagnetic coupling between Fe(II) $S = 2$ and {FeNO}^{7} $S = {}^3/_2$ centers with inclusion of zero-field splitting. Demonstration of antiferromagnetic coupling in deoxyHrNO is in line with the mounting evidence that the iron atoms in deoxyHr are weakly antiferromagnetically coupled. For deoxyHr, $-J$ has been estimated to be in the range 12–38 cm^{-1} (Reem & Solomon, 1987; Maroney et al., 1986). This estimate is dependent on the assumed magnitude and sign of the zero field splitting but is consistent with our determination of $-J \sim 23$ cm^{-1} for deoxyHrNO. The EPR-silent (semimet)$_R$HrNO and (semimet)$_O$HrNO can be similarly described as antiferromagnetically coupled Fe(III) ($S' = {}^5/_2$) and {FeNO}^{7} ($S = {}^3/_2$), giving an integer spin ground state, most likely $S^{eff} = 1$. Integer spin systems are usually EPR silent.

The Raman spectrum of deoxyHrNO exhibits resonance-enhanced modes at 433 and 421 cm^{-1}, both of which shift to lower energy upon an increase in the mass of either the nitrogen or the oxygen in the NO ligand. Since metal–ligand stretching vibrations generally give rise to more intense Raman scattering than do metal–ligand deformations, we have assigned the $\sim$3-fold more intense peak at 433 cm^{-1} as ν(Fe–N) and the 421-cm^{-1} peak as δ(Fe–N–O). The Fe–NO stretching vibration is within the range typically observed for metal–nitrosyl complexes, e.g., 370–620 cm^{-1} (Quinby-Hunt & Feltham, 1978). However, in most metal–nitrosyl complexes the δ(M–N–O) mode is more strongly affected by ^{15}NO substitution and less strongly affected by N^{18}O substitution than is the ν(M–N) mode. Such behavior has been observed, for example, with the nitrosyl complexes of hemoglobin and myoglobin (Benko & Yu, 1983). By contrast, in the spectra of deoxyHrNO the δ(Fe–N–O) and ν(Fe–N) modes undergo equivalent shifts upon exposure to either ^{15}NO or N^{18}O. A possible explanation for this discrepancy is that the Fe–NO moiety in deoxyHrNO is considerably more bent than in the other structures studied. The latter have Fe–N–O angles ranging from 180° to 130°. For example, the distorted octahedral structure of [Fe($C_9H_{21}N_3$)(NO)(N_3)$_2$], which has been shown to be an {FeNO}^{7} $S = {}^3/_2$ species, shows a Fe–N–O angle of 156° (Pohl et al., 1987). However, due to the steric constraints mentioned above, this angle in deoxyHrNO is likely to be closer to 111°, the Fe–N–N angle in azidometHr (Stenkamp et al., 1984). In synthetic complexes containing the {Fe–NO}^{7} unit, nonlinearity is typically associated with substantial transfer of electron density from the metal onto the nitrosyl group, which has the limiting Fe^{III}NO$^-$ formulation (Enemark et al., 1978). Given the probability of a small Fe–N–O angle, the bound NO in deoxyHrNO is likely to have substantial NO$^-$ character as well.

When deoxyHrNO is prepared in D_2O δ(Fe–N–O) undergoes a 7-cm^{-1} shift to lower energy with essentially no effect on ν(Fe–N). This observation is consistent with the terminal oxygen atom of the bound NO being involved in a hydrogen bond. In the crystal structure of azidometHr, the only polar group within 6 Å of the exogenous ligand binding site is the oxygen of the μ-oxo bridge (R. E. Stenkamp, personal communication). Hydrogen bonding of the bound NO in deoxyHrNO implies electron delocalization onto the terminal oxygen, supporting an [Fe^{II},Fe^{III}NO$^-$] formulation for the iron site, as suggested above. In deoxyHrNO, the most logical hydrogen-bonded structure is one in which the μ-hydroxo bridge behaves as a hydrogen-bond donor (Figure 9). In contrast, the O_2^{2-} formulation for bound dioxygen in oxyHr makes it more likely that the peroxide is protonated and serves as the hydrogen-bond donor to the μ-oxo bridge.

DeoxyHrNO undergoes slow autoxidation under anaerobic conditions, and on the basis of the optical and EPR spectra, the product appears to be an NO adduct of semimetHr. These results suggest that the autoxidation proceeds by loss of NO$^-$, thereby achieving a one-electron oxidation of deoxyHr. The excess NO present then forms an adduct with the resulting semimetHr. The proposed loss of NO$^-$ during autoxidation of deoxyHrNO parallels the loss of O_2^{2-} suggested for autoxidative conversion of oxy- to metHr (Bradić et al., 1977). Autoxidation of deoxyHrFNO is much slower. This increase in stability to autoxidation is remarkable given the spectroscopic similarities of the iron sites of deoxyHrFNO and deoxyHrNO. The hydrophobic character of the ligand binding pocket in oxygen-carrying proteins favors uptake and release of ligands such as O_2 and NO in a neutral state (Loehr, 1987). In the case of deoxyHr, a manifestation of this hydrophobicity is that binding of N_3^-, CNO^-, or F^- to the iron site is accompanied by uptake of a proton (Wilkins & Wilkins, 1987). This

hydrophobicity would tend to favor reversible binding of O_2 or NO over autoxidation via loss of O_2^{2-} or NO^-. Given this hydrophobicity and the hydrogen-bonded structure for deoxyHrNO (Figure 9), it is possible that autoxidation in this case occurs by loss of HNO.

The failure to observe the δ(Fe–N–O) mode or any deuterium isotope dependence for the ν(Fe–N) mode in deoxyHrFNO is consistent with a significant structural alteration such as a fluoride-bridged rather than hydroxide-bridged binuclear iron site. This alteration would remove the only proton donor (i.e., the μ-hydroxo bridge) from the vicinity of the iron site and make loss of HNO less likely. Lack of a nearby proton donor could thus contribute to the greater stability of deoxyHrFNO vs deoxyHrNO to autoxidation. The relatively sluggish reaction of deoxyHrFNO with O_2 suggests that other, as yet undelineated, structural and/or electronic differences also contribute to the increased stability of deoxyHrFNO vs deoxyHrNO.

Previous results from our laboratory (Nocek et al., 1984) have established that HONO is a facile one-electron oxidant of deoxyHr, that this oxidation occurs in two stages, and that the ultimate product is a nitrite adduct of semimetHr. The scheme proposed for this oxidation is

$$\underset{\text{deoxy}}{[Fe^{II}(\mu\text{-}OH^-)Fe^{II}]} + HONO \xrightarrow{k_1} \underset{(\text{semimet})_R\text{NO}}{[Fe^{III}(\mu\text{-}O^{2-})\{FeNO\}^7]} + H_2O \quad (1)$$

$$\underset{(\text{semimet})_R\text{NO}}{[Fe^{III}(\mu\text{-}O^{2-})\{FeNO\}^7]} + HONO \xrightarrow{k_2} \underset{\text{semimetNO}_2}{[Fe^{II}(\mu\text{-}OH^-)Fe^{III}NO_2^-]} + NO \quad (2)$$

Reactions 1 and 2 are both written such that there is no net charge in charge on the binuclear iron site, as proposed above for autoxidation by NO. This scheme is consistent with the absence of a deoxyHrNO EPR signal during the oxidation. NO is produced quantitatively on the protein during reaction 1 and dissociates during the rate-determining step of the slower subsequent reaction 2. A reasonable mechanism for reaction 1 begins with binding of HONO to the open coordination site on Fe2. Formation of a hydrogen bond between the hydroxyl oxygen of N-bonded HONO and the proton of the μ-hydroxo bridge in deoxyHr would facilitate loss of H_2O in the rate-determining step. This loss of H_2O would be accompanied by formation of $\{FeNO\}^6$ at Fe2. At this point rapid reduction of Fe2 by Fe1 generates the final product of reaction 1. Our failure to observe a reaction between NO and [Fe^{III},Fe^{III}]-metHr suggests that without intrasite Fe1 → Fe2 electron transfer the product of reaction 1 would not be stable. However, assuming rapid intrasite electron transferability implies that both $(\text{semimet})_R$HrNO and $(\text{semimet})_O$HrNO have the [Fe^{III},$\{FeNO\}^7$] or the limiting [Fe^{III},$Fe^{III}NO^-$] formulation. Absorption spectra obtained near the end of the first stage of the oxidation of deoxyHr by HONO (Nocek et al., 1984) resemble that in Figure 8 for $(\text{semimet})_R$HrNO. One possibility is that differences between the absorption spectra of Figure 8 represent μ-oxo-bridged [$(\text{semimet})_R$HrNO] and μ-hydroxo-bridged [$(\text{semimet})_O$HrNO] derivatives. This proposal is consistent with the resemblance of the $(\text{semimet})_R$HrNO absorption spectrum to that of anion adducts of metHr (Garbett et al., 1969) and with the [Fe^{III},$Fe^{III}NO^-$] formulation. Pearce et al. (1987a,b) have recently provided independent evidence for a μ-oxo bridge in $(\text{semimet})_R$Hr.

The apparent instability of the NO adduct of metHr may derive partially from the lack of a sufficiently strong ligand field for low-spin iron in Hr. All known $Fe^{III}NO$ complexes [$\{FeNO\}^6$ in the notation of Enemark and Feltham (1974)] are low spin and diamagnetic in the ground state. A related factor may be the strong steric preference for a bent end-on geometry at the exogenous ligand binding site of Fe2 (Stenkamp et al., 1984). $\{FeNO\}^6$ is isoelectronic with $Fe^{II}CO$, which strongly prefers a linear geometry. It is perhaps noteworthy in this context that CO does not appear to bind to Hr at any oxidation level.

Our [Fe^{II},$Fe^{III}NO^-$] formulation for the iron site of deoxyHrNO coupled with the notion that rapid intrasite [Fe1Fe2] electron transfer through the μ-oxo or μ-hydroxo ligand stabilizes semimetHrNO in reaction 1 provides analogies to putative intermediates during the intrasite two-electron transfer which must occur upon binding of O_2 to deoxyHr. As with O_2, the reversible binding of NO to the iron site occurs because of an apparent kinetic barrier to autoxidation, although this barrier appears to be higher for autoxidation of oxyHr [$t_{1/2} \sim 18.5$ h at 25 °C; Wilkins and Harrington (1983) and references cited therein]. One contribution to this latter barrier may be that autoxidation of oxyHr near neutral pH formally occurs by loss of HO_2^- and requires a change in net charge on the iron site:

$$\underset{\text{oxy}}{[Fe^{III}(\mu\text{-}O^{2-})Fe^{III}O_2H^-]} + H^+ \rightarrow \underset{\text{met}}{[Fe^{III}(\mu\text{-}O^{2-})Fe^{III}]} + H_2O_2$$

This line of reasoning is analogous to that given above for the increased stability of deoxyHrFNO vs deoxyHrNO to autoxidation.

Our results suggest that NO could be a useful probe of the growing class of non-heme binuclear iron sites in proteins, for which Hr has become the prototype. These proteins include ribonucleotide reductase B2 subunits (Sjöberg & Gräslund, 1983), porcine uteroferrin, beef spleen purple acid phosphatase (Antanaitis & Aisen, 1983; Averill et al., 1987), protein A of methane monooxygenase (Woodland et al., 1986), and the initial phases of nucleation during formation of the ferritin core (Chasteen et al., 1985).

Registry No. NO, 10102-43-9; Fe, 7439-89-6; ^{15}NO, 15917-77-8; $Na^{15}NO_2$, 68378-96-1; O_2, 7782-44-7; N_3^-, 14343-69-2; OCN^-, 661-20-1; F^-, 16984-48-8; ascorbate, 50-81-7.

References

Aasa, R., & Vanngard, T. (1975) *J. Magn. Reson. 19*, 308–315.

Abragam, C. A., & Bleaney, B. (1970) *Electron Paramagnetic Resonance of Transition Ions*, Oxford University Press, Oxford.

Antanaitis, B. C., & Aisen, P. (1983) *Adv. Inorg. Biochem. 5*, 111–136.

Arciero, D. M., Lipscomb, J. D., Huynh, B. H., Kent, T. A., & Munck, E. (1983) *J. Biol. Chem. 258*, 14981–14991.

Armstrong, G. D., & Sykes, A. G. (1986) *Inorg. Chem. 25*, 3514–3516.

Averill, B. A., Bale, J. R., & Orme-Johnson, W. H. (1978) *J. Am. Chem. Soc. 100*, 3034–3043.

Averill, B. A., Davis, J. C., Burnam, S., Zirino, T., Sanders-Loehr, J., Loehr, T. M., Sage, J. T., & Debrunner, P. G. (1987) *J. Am. Chem. Soc. 109*, 3760–3767.

Babcock, L. M., Bradić, Z., Harrington, P. C., Wilkins, R. G., & Yoneda, G. S. (1980) *J. Am. Chem. Soc. 102*, 2849–2850.

Benko, B., & Yu, N. (1983) *Proc. Natl. Acad. Sci. U.S.A. 80*, 7042–7046.

Bill, E., Bernhardt, F., Trautwein, A. X., & Winkler, H. (1985) *Eur. J. Biochem. 147*, 177–182.

Bonner, F. T. (1970) *Inorg. Chem. 9*, 190–193.

Bradič, Z., Conrad, R., & Wilkins, R. G. (1977) *J. Biol. Chem. 252*, 6069–6075.

Chasteen, N. D., Antanaitis, B. C., & Aisen, P. (1985) *J. Biol. Chem. 260*, 2926–2929.

Chrisman, B. L., & Tumolillo, T. A. (1971) *Comp. Phys. Commun. 2*, 322–330.

Dawson, J. W., Gray, H. B., Hoenig, H. E., Rossman, G. R., Schredder, J. M., & Wang, R.-H. (1972) *Biochemistry 11*, 461–465.

Enemark, J. H., & Feltham, R. D. (1974) *Coord. Chem. Rev. 13*, 339–406.

Enemark, J. H., Feltham, R. D., Huie, B. T., Johnson, P. L., & Swedo, K. B. (1978) *J. Am. Chem. Soc. 99*, 3285–3292.

Garbett, K., Darnall, D. W., Klotz, I. M., & Williams, R. J. P. (1969) *Arch. Biochem. Biophys. 135*, 419–434.

Garbett, K., Johnson, C. E., Klotz, I. M., Okamura, M. L., & Williams, R. J. P. (1971) *Arch. Biochem. Biophys. 142*, 574–583.

Gayda, J., Gibson, J. F., Cammack, R., Hall, D. O., & Mullinger, R. (1976) *Biochim. Biophys. Acta 434*, 154–163.

Hodges, K. D., Wollman, R. G., Kessel, S. L., Hendrickson, D. N., VanDerveer, D. G., & Barefield, E. K. (1979) *J. Am. Chem. Soc. 101*, 906–917.

Irwin, M. J., Duff, L. L., Shriver, D. F., & Klotz, I. M. (1983) *Arch. Biochem. Biophys. 224*, 473–478.

Klotz, I. M., & Kurtz, D. M., Jr. (1984) *Acc. Chem. Res. 17*, 16–22.

Klotz, I. M., Klotz, T. A., & Fiess, H. A. (1957) *Arch. Biochem. Biophys. 68*, 284–289.

Kurtz, D. M., Jr. (1986) in *Invertebrate Oxygen Carriers* (Linzen, B., Ed.) pp 9–21, Springer-Verlag, New York.

Loehr, T. M. (1987) in *Oxygen Complexes and Oxygen Activation by Metal Complexes* (Martell, A. E., Ed.) Plenum, New York (in press).

Maroney, M. J., Kurtz, D. M., Jr., Nocek, J. M., Pearce, L. L., & Que, L., Jr. (1986) *J. Am. Chem. Soc. 108*, 6871–6879.

Mino, Y. M., Loehr, T. M., Wada, K., Matsubara, H., & Sanders-Loehr, J. (1987) *Biochemistry 26*, 8059–8065.

Muhoberac, B. B., Wharton, D. C., Babcock, L. M., Harrington, P. C., & Wilkins, R. G. (1980) *Biochim. Biophys. Acta 626*, 337–345.

Nocek, J. M., Kurtz, D. M., Jr., Pickering, R. A., & Doyle, M. P. (1984) *J. Biol. Chem. 259*, 12334–12338.

Nocek, J. M., Kurtz, D. M., Jr., Sage, J. T., Debrunner, P. G., Maroney, M. J., & Que, L., Jr. (1985) *J. Am. Chem. Soc. 107*, 3382–3384.

Okamura, M. Y., Klotz, I. M., Johnson, C. E., Winter, M. R. C., & Williams, R. J. P. (1969) *Biochemistry 8*, 1951–1958.

Pearce, L. L., Kurtz, D. M., Jr., Xia, Y.-M., & Debrunner, P. G. (1987a) *J. Am. Chem. Soc. 109*, 7286–7293.

Pearce, L. L., Utecht, R. E., & Kurtz, D. M., Jr. (1987b) *Biochemistry 26*, 8709–8717.

Pohl, K., Wieghardt, K., Nuber, B., & Weiss, J. (1987) *J. Chem. Soc., Dalton Trans.*, 187–192.

Quinby-Hunt, M., & Feltham, R. D. (1978) *Inorg. Chem. 17*, 2515–2520.

Ram, M. S., & Stanbury, D. M. (1984) *J. Am. Chem. Soc. 106*, 8136–8142.

Reem, R. C., & Solomon, E. I. (1984) *J. Am. Chem. Soc. 106*, 8323–8325.

Reem, R. C., & Solomon, E. I. (1987) *J. Am. Chem. Soc. 109*, 1216–1226.

Rutter, R., Hager, L. P., Dhonau, H., Hendrich, M., Valentine, M., & Debrunner, P. (1984) *Biochemistry 23*, 6809–6816.

Sage, J. T., & Debrunner, P. G. (1986) *Hyperfine Interact. 29*, 1399–1402.

Shiemke, A. K., Loehr, T. M., & Sanders-Loehr, J. (1984) *J. Am. Chem. Soc. 106*, 4951–4956.

Shiemke, A. K., Loehr, T. M., & Sanders-Loehr, J. (1986) *J. Am. Chem. Soc. 108*, 2437–2443.

Sieker, L. C., Stenkamp, R. E., & Jensen, L. H. (1982) in *The Biological Chemistry of Iron* (Dunford, H. B., Dolphin, D., Raymond, K. N., & Sieker, L. C., Eds.) pp 161–175, Reidel, New York.

Sjöberg, B. M., & Gräslund, A. (1983) *Adv. Inorg. Biochem. 5*, 87–110.

Sjöberg, B. M., Loehr, T. M., & Sanders-Loehr, J. (1982) *Biochemistry 21*, 96–102.

Spool, A. (1985) Ph.D. Dissertation, Massachusetts Institute of Technology.

Stenkamp, R. E., Sieker, L. C., & Jensen, L. H. (1984) *J. Am. Chem. Soc. 106*, 618–622.

Stenkamp, R. E., Sieker, L. C., Jensen, L. H., McCallum, J. D., & Sanders-Loehr, J. (1985) *Proc. Natl. Acad. Sci. U.S.A. 82*, 713–716.

Wells, F. V., McCann, S. W., Wickman, H. H., Kessel, S. L., Hendrickson, D. W., & Feltham, R. D. (1982) *Inorg. Chem. 21*, 2306–2311.

Wertz, J. E., & Bolton, J. R. (1972) *Electron Spin Resonance. Elementary Theory and Practical Applications*, pp 450–466, McGraw-Hill, New York.

Wilkins, R. G., & Harrington, P. C. (1983) *Adv. Inorg. Biochem. 5*, 51–85.

Wilkins, R. G., & Wilkins, P. C. (1987) *Biochim. Biophys. Acta 912*, 48–55.

Woodland, M. P., Davlat, S. P., Cammack, R., & Dalton, H. (1986) *Biochim. Biophys. Acta 873*, 237–242.

Yim, M. B., Kuo, L. C., & Makinen, M. W. (1982) *J. Magn. Reson. 46*, 247–256.